

See discussions, stats, and author profiles for this publication at: <https://www.researchgate.net/publication/228068805>

Chemical Waves in the Iodide–Nitric Acid System

ARTICLE *in* THE JOURNAL OF PHYSICAL CHEMISTRY · JUNE 1994

Impact Factor: 2.78 · DOI: 10.1021/j100074a033

CITATIONS

31

READS

19

5 AUTHORS, INCLUDING:



Istvan Nagy

University of Debrecen

33 PUBLICATIONS 597 CITATIONS

[SEE PROFILE](#)



John Pojman

Louisiana State University

238 PUBLICATIONS 4,134 CITATIONS

[SEE PROFILE](#)



György Bazsa

University of Debrecen

24 PUBLICATIONS 208 CITATIONS

[SEE PROFILE](#)



Zoltan Noszticzius

Budapest University of Technology and Econ...

99 PUBLICATIONS 1,840 CITATIONS

[SEE PROFILE](#)

Chemical Waves in the Iodide–Nitric Acid System

Istvan P. Nagy,^{†,‡} Andrea Keresztesy,[‡] John A. Pojman,^{*}[†] György Bazsa,[‡] and Zoltan Noszticzius[§]

Department of Chemistry and Biochemistry, University of Southern Mississippi, Hattiesburg, Mississippi 39406-5043; Department of Physical Chemistry, Kossuth Lajos University, Debrecen, Hungary H-4010; and Institute of Physics, Technical University of Budapest, H-1521 Budapest, Hungary

Received: November 29, 1993; In Final Form: April 12, 1994[¶]

Chemical waves can be observed during the oxidation of iodide by 3–4.5 M nitric acid. The rate of the wave propagation and the wave shape under convection-free and convective conditions were studied using tubes with different diameters and at varying orientations to the gravitational vector. The activation energy of the reaction-diffusion front was determined. For the homogeneous reaction, the isothermal density change ($\Delta\rho_c$) was measured and found to be negative. Because the reaction is exothermic, the Pojman and Epstein analysis of convective stability predicted only simple convection could occur. However, double-diffusive convection and fingering were observed. With special convection cells fed through permeable membranes we proved that double-diffusive convection could occur by having two solutal species (iodide and triiodide-starch complex) with significantly different diffusion coefficients and not only from competing thermal and solutal density changes. A mechanism for the angular dependence of the gravitational anisotropy in front velocities is proposed in terms of the Boycott effect.

Introduction

An autocatalytic reaction in an unstirred vessel can support a constant-velocity wave front resulting from the coupling of diffusion to the chemical reaction. Numerous reactions in solution have been described in which a front of chemical reactivity propagates through the medium from the site of an initial concentration perturbation.^{1–11}

As a front propagates, concentration and thermal gradients are formed that alter the density of the solution, often causing convection.^{5,11–18} Pojman and Epstein¹⁹ proposed a classification of the types of convection that can occur in traveling fronts based on the relative signs of the thermally induced density change ($\Delta\rho_T$) and the density change caused by the change in composition ($\Delta\rho_c$). If the reaction is exothermic ($\Delta\rho_c < 0$) and the products' solution is less dense than the reactants' ($\Delta\rho_c < 0$), then simple convection can occur, depending on the constraints of the container geometry. If the signs of $\Delta\rho_c$ and $\Delta\rho_T$ are not the same, then multicomponent (double-diffusive) convection may occur, even though the overall density gradient may appear to be stable. In a descending front, double-diffusive convection manifests itself as “salt fingers”, so-called because of their discovery in ocean layer mixing.²⁰

If a front of an exothermic reaction whose $\Delta\rho_c > 0$ propagates downward, then the system may appear to be stable to buoyancy-induced convection. In fact it is not. To understand how convection can occur, we must consider an analogous configuration with both salt and thermal gradients. Consider hot, salty water above cold, fresh water as depicted in Figure 1a. The system appears to be stable if $\Delta\rho_c + \Delta\rho_T = 0$ (no net density gradient). Yet, it may not be. Imagine that, at the interface between the layers, a small parcel of the upper solution were to deviate from its position by gradually enlarging and descending into the cold, fresh region. Because the temperature and concentration are higher than in the surrounding region, heat and salt will diffuse out. The heat will leave at a greater rate, because of the larger diffusivity of heat (by 2 orders of magnitude). Now the parcel is cool and dense; because of its higher concentration, it sinks.

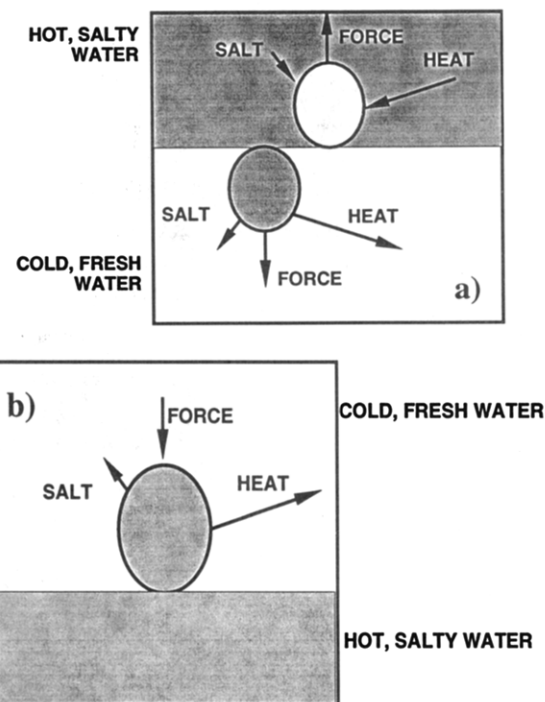


Figure 1. (a) Mechanism for double-diffusive convection in the fingering regime. $\Delta\rho_c$ and $\Delta\rho_T$ have opposite signs, and the net density gradient appears to be stable. However, if a small parcel of the warm, salty solution enters the lower section, because the heat diffuses faster than the salt, the parcel is left with a greater density than the surrounding medium. The buoyant force pulls it down. If a small parcel of cold, fresh water enters the warm, salty solution, heat will diffuse in faster than the salt. The parcel will be less dense than its surroundings and rise. (b) Mechanism for double-diffusive convection in the diffusive regime. The parcel of hot, salty solution that enters the cold, fresh region above loses heat, becoming more dense than the surrounding region. It sinks back to the hot region and regains heat.

Similarly, if a parcel of cold, fresh water protrudes into the hot, salty layer, heat will diffuse in faster than the salt. This will leave the parcel less dense than the surrounding layer, and the parcel will rise. What results are known as “salt fingers”, which appear as long slender regions of alternately descending and

[†] University of Southern Mississippi.

[‡] Kossuth Lajos University.

[§] Technical University of Budapest.

[¶] Abstract published in *Advance ACS Abstracts*, May 15, 1994.

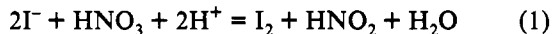
ascending fluid.^{21,22} If cold, fresh water overlies denser, hot, salty water, the system is still statically stable. However, we again must consider a perturbation at the interface, as depicted in Figure 1b. The heat diffuses faster than the salt, leaving the parcel heavier than the surrounding region. It sinks and can continue through the interface into the hot, salty region, where it again heats up and rises. This oscillatory behavior will continue as long as the density gradients persist. This oscillatory process increases the effective area of the interface, thereby increasing the flux of salt. The heat released into the region above the interface causes convection, which further increases the mass transport. Both of the above types of convection are categorized as “double-diffusive” convection (“thermohaline” when the two components are salt and heat) and more generally as “multicomponent convection”.^{21,22} It is not necessary that the two components be a solute and heat. Any two materials with different diffusivities can cause these phenomena, even if the differences are small as with salt and sugar, or with polymer solutions of different molecular weight distributions.²³ This phenomenon has been extensively studied by oceanographers because of the role it plays in ocean current mixing.^{21,24–28} It has also been shown to cause pattern formation in some photochemical reactions.²⁹ The two behaviors we have described correspond to the “fingering” and “diffusive” regimes of double-diffusive convection, respectively.

Chemical waves existing in the iodate–arsenous acid system were studied by Pojman et al. and found to exhibit simple convection, in which the ascending fronts propagated faster than the descending fronts if the tube radius was greater than a critical value.¹³ The descending fronts had the same velocity as a pure reaction–diffusion front and were flat. The ascending fronts with convection had parabolic shapes. The iron–nitric acid system was studied by Bazsa and Epstein and found to exhibit a gravitationally induced anisotropy in front propagation, in which both ascending and descending fronts could propagate faster than a pure reaction–diffusion front.⁵ Pojman et al. determined the system was exhibiting double-diffusive convection because $\Delta\rho_c$ was positive and $\Delta\rho_T$ was negative.¹² The fronts of the chlorate oxidation of sulfite were recently found to exhibit multicomponent convection.³⁰

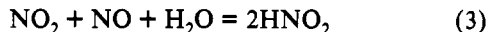
We set out to study chemical waves in the iodide–nitric acid system because even though $\Delta\rho_c$ and $\Delta\rho_T$ are negative, both ascending and descending fronts can propagate faster than the pure reaction–diffusion front, and pronounced convective fingering can be seen in large tubes. We found that the Pojman–Epstein model does not adequately predict the behavior of this system because another type of double-diffusive convection can occur if there are large differences in the values of diffusion coefficients of solutal species. The presence of starch plays a key role in affecting the diffusion coefficient of the triiodide.

The Iodide–Nitric Acid Reaction

The oxidation of iodide was studied by Eckstädt³¹ at the beginning of the century. He successfully determined the stoichiometry (eq 1) but found the kinetics irreproducible. More



recently, Nagy and Bazsa³² investigated the kinetics under batch conditions and found that the irreproducible kinetics were caused by microscopic inhomogeneities initiating chemical waves on the surface of the reaction vessel or the Teflon stir bar. The reaction is autocatalytic in HNO_2 , which is formed during the reaction with traces of the NO .³³



This system can support a single wave (front) of iodide oxidation.

Experimental Section

Chemicals and Apparatus. Reactant solutions were prepared with analytical grade chemicals (REANAL) and distilled water. The HNO_3 solutions were diluted from concentrated nitric acid. Before each experiment, traces of NO_2 , NO , and oxygen were removed by bubbling with argon for 1 h. Iodine stock solutions were prepared by measuring the stoichiometric ratios of NaI and KIO_3 in a mildly acidic solution. The exact iodine concentration was checked both by titration with $Na_2S_2O_3$ solution and spectrophotometry.

To achieve convection-free conditions, we used CAB-O-SIL fumed silica (Cabot Corp., particle size 0.007–0.027 μm , refractive index 1.46), which forms a stable gel even in a 10 M HNO_3 solution. Wave experiments were carried out using pipets and glass tubes with various inside diameters (up to 2.4 cm). The temperature was controlled by a custom air thermostat. Wave position was read from a millimeter scale attached to the wall of the tube. Determinations of reaction enthalpies were carried out using a Dewar flask and a Beckmann differential thermometer. Reaction mixture densities were measured in a 10-mL pycnometer.

Wave Velocity Measurements. Standard stock solutions and distilled water were pipetted in appropriate volumes to give reaction mixtures of desired concentrations. A proper amount of $N_2H_4SO_4$ was added to each of the mixtures to quench species that are considered autocatalysts of the iodide oxidation and formed by the slow self-decomposition of the mixture (HNO_2 , NO_2 , NO). In the case of the convection-free conditions CAB-O-SIL was added to form a 1.5 w/w % stable gel. Capillary tubes were carefully cleaned and dried with acetone. After filling up the tube, NO_2 gas was blown from a 5-mL syringe over the end of the capillary to initiate the wave. Wave shapes were captured by a digital image processing system that consisted of an IBM 80-386/387 compatible PC, an LFS-AT 8 bit black and white frame grabber board (LEUTRON AG, Switzerland), and an SDT 4500 monochrome CCD solid-state camera (Steiner DataTechnik GmbH, Germany) and the necessary optics (25-nm-focal length TOKINA lenses, Japan).

Determination of the Reaction Heat and the Isothermal Density Change. Appropriate volumes of stock solutions were combined to give a 200.0-mL reaction mixture that was poured into a Dewar flask, and the temperature was monitored for 10 min. The reaction was started in the same manner as it was done in the case of the wave velocity measurements. The temperature increase was measured while the solution turned brown. The temperature change using 0.002 M initial iodide concentration was 0.005–0.008 °C, and the $\Delta H = -130 \pm 10 \text{ kJ/mol}$.

The reaction density change was determined under the same conditions as the wave velocity experiments. An unreacted mixture was measured using a 10-mL nominal volume pycnometer. The isothermal density change was found to be $\Delta\rho_c = -5 \times 10^{-4} \text{ g/cm}^3$.

Convection Cells Used in the Experiments. The cells described below were used to study both reactive and unreactive systems. To yield information on the fluid motion’s behavior in the 0.2–5-s time scale, we used a cell shown in Figure 2a and described by Pota et al.³⁴ The cell is made of Plexiglas with a 1- × 1-cm square hole between two chambers. An impermeable membrane is placed between the chambers. To bring the two solutions into contact with each other, the membrane is pulled out.

The second type of the reactor used is a Hele-Shaw-type convection cell developed by Predtechensky et al.³⁵ The reactor shown in Figure 2b consists of three sections separated by permeable membranes. The upper and lower sections were machined to have chambers in direct contact with the membranes

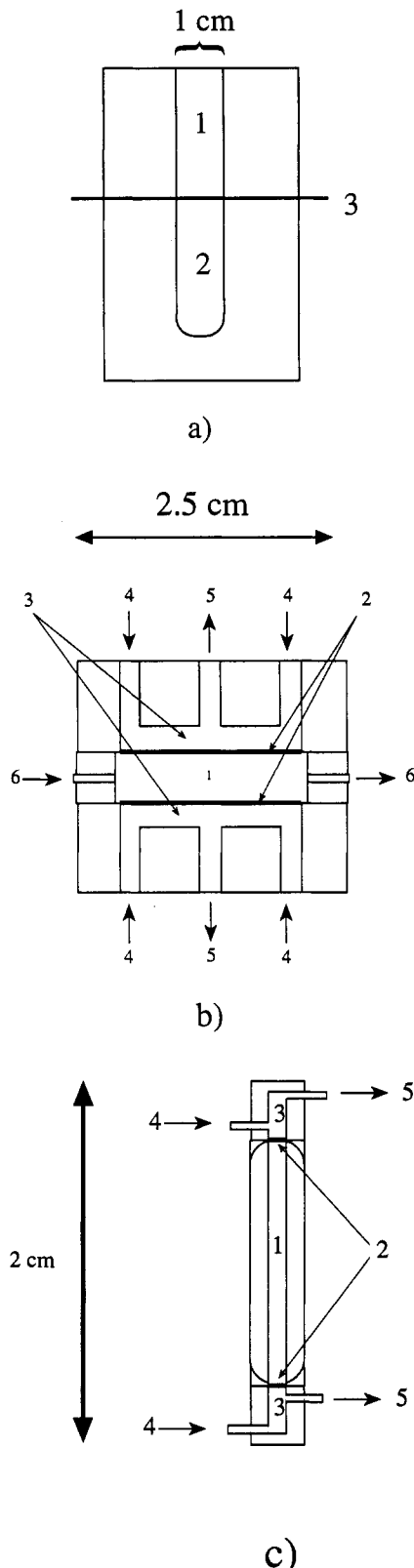


Figure 2. Reactors used for model systems to investigate the fluid motion under unreactive conditions. (a) Pseudowave cell: 1, 2, half cells; 3, impermeable plastic membrane; (b) membrane-equipped Hele-Shaw-type convection cell, and (c) tubular membrane reactor: 1, reactive cell; 2, permeable or semipermeable membrane; 3, half cells fed by peristaltic pump; 4, inflow channel; 5, outflow channel; 6, capillaries to fill up the reactive chamber with an initial solution.

and holes for reactant inflows and outflows. Material flux to the midsection cell is allowed only by pure diffusion, and if any reaction takes place in the cell, the products can exit only by diffusion. The two half cells of the membrane-equipped Hele-Shaw-type

TABLE 1: Rate of Convection-Free Front Propagation as a Function of the Nitric Acid Concentration^a

[HNO ₃] ₀ (M)	3.0	3.5	4.0	4.5
velocity (cm/min)	0.015 ± 0.001	0.0242 ± 0.0004	0.0388 ± 0.0004	0.048 ± 0.0005

^a $T = 21.5 \pm 0.5^\circ\text{C}$, $[\text{KI}]_0 = 0.002 \text{ M}$; $[\text{N}_2\text{H}_6\text{SO}_4]_0 = 2 \times 10^{-4} \text{ M}$; [starch] = 0.2 m/v %.

TABLE 2: Rate of Convection-Free Front Propagation as a Function of the Initial Iodide Concentration^a

[KI]₀ (M)	0.002	0.003	0.004
velocity (cm/min)	0.0385 ± 0.0002	0.020 ± 0.001	0.0237 ± 0.0009

^a $T = 21.5 \pm 0.5^\circ\text{C}$, $[\text{HNO}_3]_0 = 4.0 \text{ M}$; $[\text{N}_2\text{H}_6\text{SO}_4]_0 = 2 \times 10^{-4} \text{ M}$; [starch] = 0.2 m/v %.

TABLE 3: Rate of Front Propagation as a Function of the Temperature in Gel^a

temperature (°C)	21.5 ± 0.05	30.5 ± 0.5	38.5 ± 0.5
velocity (cm/min)			
ascending	0.014 ± 0.001	0.030 ± 0.001	0.049 ± 0.001

^a $[\text{HNO}_3]_0 = 3.0 \text{ M}$; $[\text{KI}]_0 = 0.002 \text{ M}$; $[\text{N}_2\text{H}_6\text{SO}_4]_0 = 2 \times 10^{-4} \text{ M}$; [starch] = 0.2 m/v % with 1–4 m/m % CAB-O-SIL.

convection cell were fed by a DESAGA PLG 132100 peristaltic pump. The third type is a tubular membrane reactor (Figure 2c), which is similar to the Hele-Shaw cell except the horizontal chamber is replaced with thin tubing. With this reactor we used a RAININ Rabbit-Plus peristaltic pump. In all experiments we used SIGMA dialysis tubing, No. D-9777.

Although the nitric acid was in great excess in our experiments, only about 90% of the iodide was reacted, leaving enough to form the triiodide complex. The triiodide-starch complex formed in a front can slowly precipitate and settle. This was not a problem with front experiments because the fronts propagate on a faster time scale but could have an impact on the model systems.

Results

Wave Velocity Dependence on Initial Concentrations under Convection-Free Conditions. The basic aim of the experiments carried out was to study convective phenomena arising in the iodide-nitric acid system, but it is also important to know what is the contribution to the wave propagation of the pure reaction-diffusion front. We used 0.270-cm-i.d. tubing filled with the necessary amount of reactant mixture mixed together with CAB-O-SIL to form a viscous gel. Waves propagated smoothly with a constant speed, in ascending and descending directions; no significant reaction occurred outside the front during the course of an experiment.

We studied the initial iodide and nitric acid concentration dependences of the ascending and descending convection-free fronts. Because there were no significant differences between the ascending and descending cases, the data were combined and are reported in Tables 1 and 2. Under convection-free conditions the wave propagation speed is increased by increasing the initial nitric acid concentration but shows a minimum at 0.003 M KI. We do not have an explanation for such behavior but note that it is reproducible in both the convection-free and convective (Table 5) fronts.

Temperature Dependence of the Velocity. We investigated the temperature dependence of the velocity of the pure reaction-diffusion front in both ascending and descending directions. Results obtained using a fixed set of initial reactant concentrations are shown in Table 3.

Increasing the temperature increases the ascending and descending front velocity. The velocities are slightly different in the ascending and descending cases, especially at 38.5 °C. This

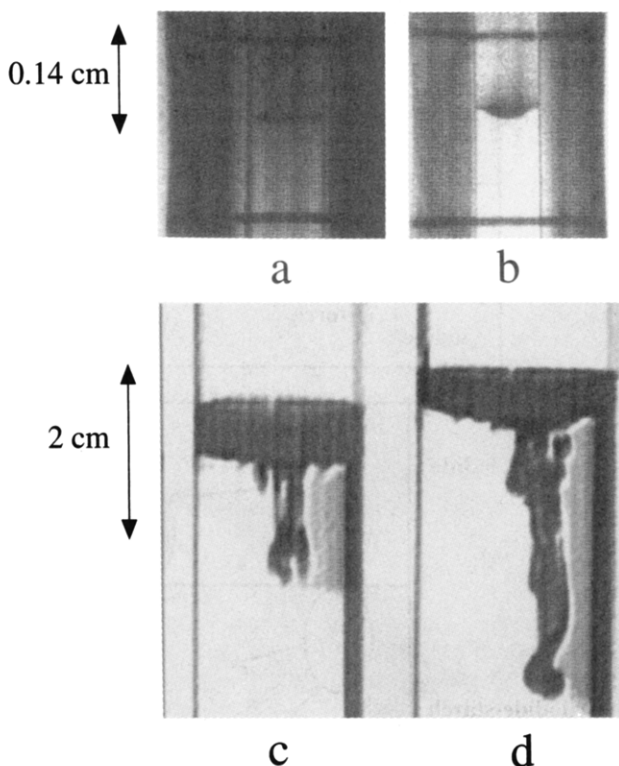


Figure 3. Shapes of the propagating fronts, without CAB-O-SIL. All fronts consist of a bluish-black region that propagates as a single front; (a) ascending and (b) descending directions in a 0.140-cm-i.d. capillary tube; (c) and (d) fingering during descending propagation in a 2.00-cm-i.d. tube. $[HNO_3]_0 = 3.0\text{ M}$; $[KI]_0 = 0.002\text{ M}$; $[N_2H_6SO_4]_0 = 2 \times 10^{-4}\text{ M}$; [starch] = 0.2 m/v %.

fact can be related to the viscosity change of the gelled medium. It means that we are close to the gelation concentration, where convection could have a small role because of the decrease in viscosity with temperature.

Using the data of Table 3, we calculated the activation energy of the pure reaction–diffusion front to be $57 \pm 1.5\text{ kJ/mol}$ for the ascending case and $62 \pm 1.5\text{ kJ/mol}$ for the descending case. These values are close enough to each other to be considered as a good approximation for the activation energy of the pure reaction–diffusion front. This is a reasonable result given that redox reactions involving iodide normally have activation energies of $35\text{--}55\text{ kJ/mol}$, e.g., $47 \pm 1\text{ kJ/mol}$ for the iodide–persulfate reaction.³⁶ The activation energy of diffusion in aqueous solutions is not larger than 20 kJ/mol .

Effect of Initial Concentrations, Orientation, and Temperature in Capillary Tubes with Convection. Using the reaction mixture of $[HNO_3]_0 = 3.0\text{ M}$, $[KI]_0 = 0.002\text{ M}$, $[N_2H_6SO_4]_0 = 2 \times 10^{-4}\text{ M}$, and [starch] = 0.2 m/v %, we performed experiments in vertical tubes having inner diameters of 0.140, 0.270, 0.390, and 0.800 cm. With ascending fronts at all diameters a flat-shaped regime formed after the initiation with NO_2 gas. In the case of larger diameters, after a few millimeters propagation the shape became asymmetric and distorted by convection; the 0.140-cm tube supported a flat front during the entire propagation.

Experiments with descending fronts regularly showed a parabolic shape immediately after the initiation, but the larger diameter cases were found to be unstable; only the 0.140-cm-diameter tube supported a stable parabolic shape during the entire propagation. If the tube diameter was over 1.5 cm, fingering occurred immediately after the initiation. Representative wave shapes in small and large diameter tubes are shown in Figure 3.

Using the 0.140-cm-i.d. tube, we studied the effect of initial nitric acid and iodide concentrations on the front velocity. The results for 2–3 parallel runs are listed in Tables 4 and 5.

It can be unambiguously claimed that the velocities in all cases

TABLE 4: Rate of Front Propagation with Convection as a Function of the Nitric Acid Concentration^a

$[HNO_3]_0\text{ (M)}$	3.0	3.5	4.0	4.5
velocity (cm/min)				
ascending	0.021 ± 0.001	0.044 ± 0.002	0.043 ± 0.004	0.070 ± 0.004
descending	0.24 ± 0.02	0.245 ± 0.006	0.227 ± 0.003	0.25 ± 0.02

^a $T = 23.5 \pm 0.5\text{ }^\circ\text{C}$; $[KI]_0 = 0.002\text{ M}$; $[N_2H_6SO_4]_0 = 2 \times 10^{-4}\text{ M}$; [starch] = 0.2 m/v %.

TABLE 5: Rate of Front Propagation with Convection as a Function of the Initial Iodide Concentration^a

$[KI]_0\text{ (M)}$	0.002	0.003	0.004
velocity (cm/min)			
ascending	0.046 ± 0.003	0.026	0.030 ± 0.001
descending	0.224	0.226 ± 0.006	0.27 ± 0.01

^a $T = 23.5 \pm 0.5\text{ }^\circ\text{C}$, $[HNO_3]_0 = 4.0\text{ M}$; $[N_2H_6SO_4]_0 = 2 \times 10^{-4}\text{ M}$; [starch] = 0.2 m/v %.

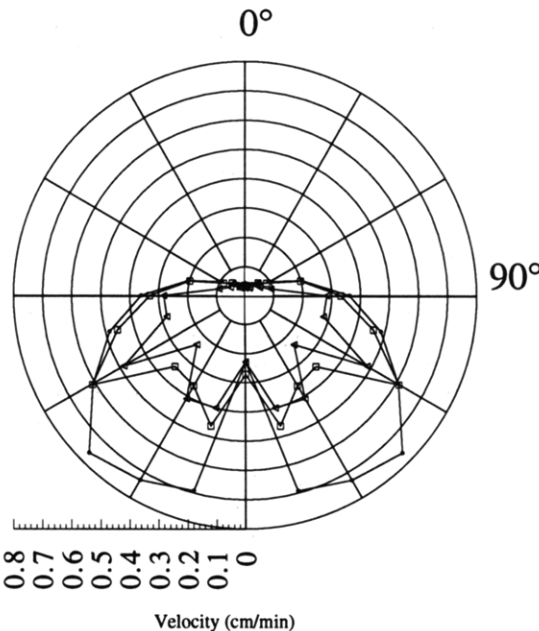


Figure 4. Polar coordinate plots of the gravitational anisotropy phenomenon observed with three different initial iodide concentrations: front velocities versus tube orientations. $T = 23.5 \pm 0.5\text{ }^\circ\text{C}$, $[HNO_3]_0 = 4.0\text{ M}$; $[N_2H_6SO_4]_0 = 2 \times 10^{-4}\text{ M}$; [starch] = 0.2 m/v %. $[KI]_0 = 0.002\text{ M}$; 0.003 M ; 0.004 M ; 0° indicates the vertical ascending direction, and 180° is the vertical descending direction.

are larger than in the presence of CAB-O-SIL. The difference in the case of descending fronts is close to an order of magnitude. These observations are consistent with the gravitational anisotropy phenomenon discovered and described in the iron(II)–nitric acid system by Bazsa and Epstein.⁵ Figure 4 shows the results at three different initial iodide concentrations and at 13 different orientations in 1.40-mm-i.d. tube. The data for this figure are included in the supplementary material. (See paragraph at end of paper regarding supplementary material.)

We also captured pictures of the ascending and descending wave shapes at five orientations, which are shown in Figure 5. The 150° and 120° cases have an asymmetric parabolic shape. The horizontally propagating front is flat and tilted 45° to the direction of propagation.

Discussion and Model System Experiments

The thermal density change ($\Delta\rho_T < 0$) and the isothermal density change ($\Delta\rho_c < 0$) have the same sign. According to the Pojman–Epstein model, simple convection should occur as in the

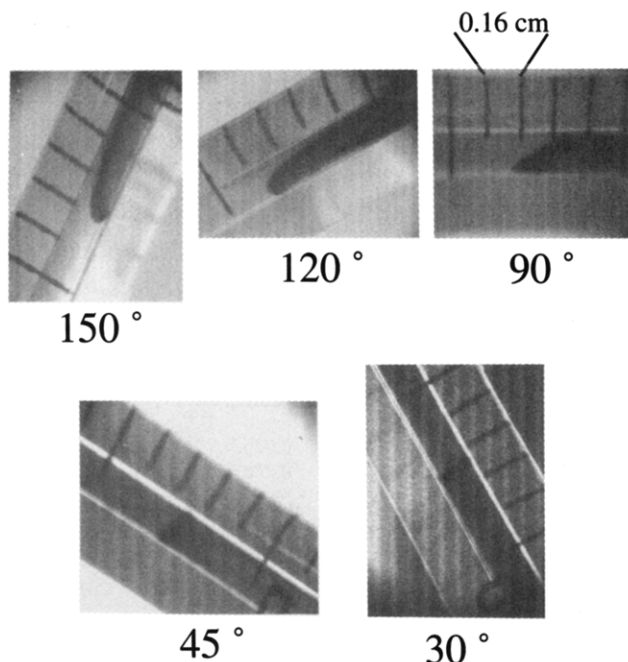


Figure 5. Shapes of propagating fronts (with convection) at five different orientations to the gravitational field. A vertical ascending front is at 0°; vertical descending is at 180°. Initial conditions are the same as in Figure 4.

iodate–arsenous acid system.¹³ However, the wave shapes for the ascending and descending fronts are opposite; in the iodate–arsenous acid system the descending front is flat and the ascending one has a parabolic shape, while in the iodide–nitric acid system the descending is parabolic and the ascending is flat (for narrow tubes). In this latest case, only simple convection would be expected, but with larger tube diameters double-diffusive convection was also observed. If simple convection were the only mechanism for fluid motion, then the descending front velocity would be the same as the pure reaction–diffusion velocity.

The thermal gradient (with ΔT of 0.005–0.008 °C) in the iodide–nitric acid system is much smaller than in the iodate–arsenous acid system, with $\Delta T = 0.7$ °C. The analysis of Pojman et al.¹³ determined that the thermal gradient played no significant role as long as $\Delta\rho_c < 0$. The isothermal volume changes are comparable in both systems.

These facts suggest that there is another mechanism for the double-diffusive convection seen in the iodide–nitric acid system than previously proposed. Such a mechanism can be provided by two species having relatively large differences in their diffusion constants, as described by Turner.²² In this case, if we consider the basic model system described by the Pojman–Epstein model, we can use an isothermal system with two layers of different but isopycnic solutions containing two species with different diffusion coefficients, such as salt and sugar. The faster diffusion from one layer provides greater material flux to the layer with the less mobile component than the reverse direction diffusion; a local density change occurs that can initiate fluid motion (Figure 6a). This mechanism can create similar conditions for double-diffusive convection as the case of the hot, salty water and cold, fresh water interface. If the considerations mentioned above are true, we should find fingering even under unreactive conditions if we have the same key species as in the iodide–nitric acid system. The potential candidates for this purpose are the iodine–starch complex and iodide.

This mechanism can operate if the layers are reversed (Figure 6b). Fingering would not occur, but an increase in the mass transport would occur across the interface as described in Figure 1b for the diffusive regime. The mass transport increase would not be as great as for the fingering regime. This is consistent

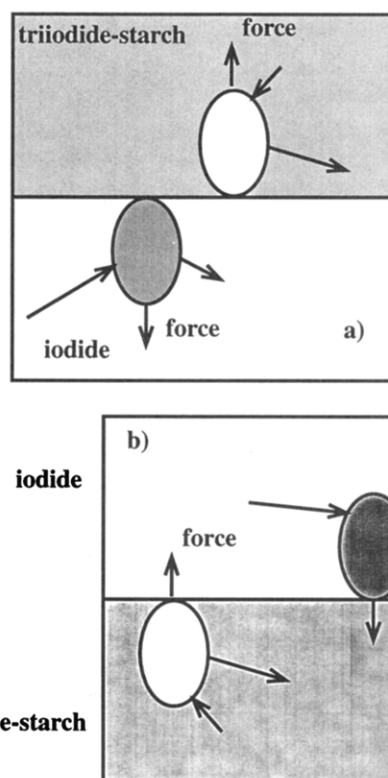


Figure 6. Mechanism for double-diffusive convection. (a) Two isopycnic layers are composed of species with different diffusion coefficients. If a small parcel of the triiodide–starch solution enters the lower section, because the iodide can diffuse in faster than the triiodide–starch can diffuse out, the parcel is left with a greater density than the surrounding medium. The buoyant force pulls it down. If a small parcel of iodide solution enters the upper solution, iodide will diffuse out faster than the triiodide–starch can diffuse into the parcel. The parcel will be less dense than its surroundings and rise. (b) Mechanism for double-diffusive convection in the diffusive regime. The parcel of triiodide–starch solution enters the iodide solution above. Iodide diffuses in more rapidly than the triiodide–starch can diffuse out, causing the parcel to become more dense than the surrounding region. It sinks back to the lower region where iodide can diffuse out, decreasing its density.

with the fact that both ascending the descending fronts propagate faster than the pure reaction–diffusion fronts, but the ascending fronts are slower than the descending fronts. Similar behavior was observed in the iron–nitric acid system, which does demonstrate double-diffusive convection.¹²

Fluid Motion Modeling in Unreactive Systems. If we have a solution of the iodine–starch complex on top of one containing iodide with the same density and temperature, we can observe double-diffusive convection (fingering) when the liquids are brought into contact. The diffusion of the iodide from the bottom solution is much faster than the diffusion of the starch-containing species, so the boundary becomes diffuse and more dense in the side of the starch-containing system, and descending fingers can occur. When the starch-containing solution is situated under the iodide solution, the faster iodide diffusion increases the density at the lower boundary. The resulting density gradient is stable so that a sharp interface should remain.

To test these predictions, we prepared two solutions containing sodium nitrate (instead of HNO_3) and starch; iodine was added to one and iodide added to the other. The densities of the two solutions were adjusted to the same density, within the error of the pycnometer. We carried out an experiment filling up the bottom of the cell described in Figure 2a with the iodide-containing solution. After closing the slit between the two half cells with an impermeable plastic membrane, the upper half cell was filled with the iodine–starch complex containing solution. With a sudden removal of the membrane a fingering zone formed (Figure 7). The time scale of the mixing of the solutions by vigorous

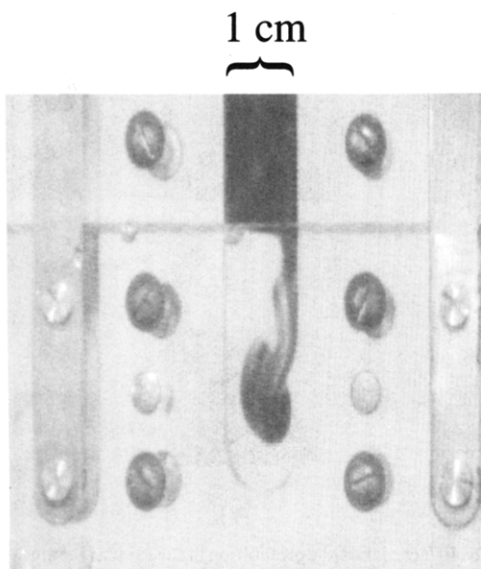


Figure 7. Fingering arising in unreactive system. Concentrations in the two half-cells before the experiment. Upper half cell: $[I_2] = 0.001\text{ M}$; $\text{NaNO}_3 = 1.550\text{ M}$; $[\text{N}_2\text{H}_4\text{SO}_4] = 2 \times 10^{-4}\text{ M}$; [starch] = 0.2 m/v %. Bottom half cell: $[I^-] = 0.002\text{ M}$; $\text{NaNO}_3 = 1.550\text{ M}$; $[\text{N}_2\text{H}_4\text{SO}_4] = 2 \times 10^{-4}\text{ M}$; [starch] = 0.2 m/v %.

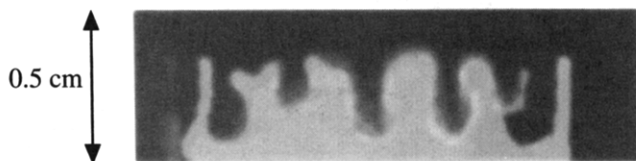


Figure 8. Structure formed in the membrane-equipped Hele-Shaw-type convection cell. Upper solution consists of 0.033 M I_2 , 0.3 M KI, and 0.5 M NaNO_3 ; lower solution consists of 0.36 M KI.

fingering was approximately 6–7 s. In the case of a reactive system, when fingering was observed in 2.0-cm-i.d. tube during descending wave propagation, the formation and complete development of fingering over the whole reaction space was observed in 9–12 s.

We repeated the unreactive experiment by reversing the initial conditions; the lower cell was filled with iodine–starch solution and the upper cell with iodide solution. After the removal of the membrane, a sharp boundary formed between the colored lower and colorless upper solutions; the boundary remained stable during 30 min of observation.

To eliminate any possible disturbance caused by the removal of the membrane, we used another reactor described by Predtechensky et al.³⁵ This device is a Hele-Shaw-type cell, which allows the reactants to meet only by diffusion through two semipermeable membranes. We prepared three solutions: (1) 0.033 M iodine, 0.3 M potassium iodide and 0.5 M NaNO_3 , (2) 0.366 M iodide, and (3) starch (0.2 m/v %). Solutions 2 and 3 were adjusted to the density of solution 1 by the addition of NaNO_3 .

The upper chamber of the horizontally positioned cell was fed with solution 1 while solution 2 was circulated through the bottom chamber. The middle section had been filled with the starch solution. (Note: the membranes were highly permeable to small molecules but effectively impermeable for macromolecules such as starch.) After 40 min, fingering patterns flowed down into the 5-mm-wide midsection of the reactor from the surface of the upper semipermeable membrane, which indicated that the iodide ions from the bottom chamber quickly diffused up and reached the slowly diffusing triiodide–starch complex. After a half an hour, a long fingering zone appeared, which is shown in Figure 8. This structure remained stable for 15–20 min until the triiodide zone reached the bottom membrane.

We carried out an experiment using the opposite arrangement for feeding the reactor. A temporarily sharp boundary in the

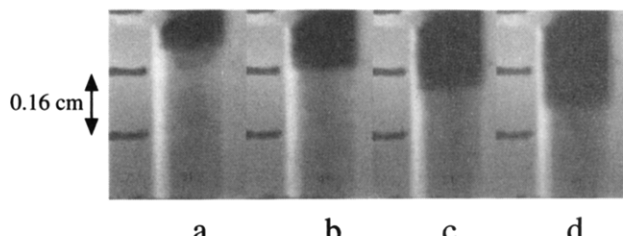


Figure 9. Slow descending wave propagation observed in tubular membrane reactor. Times of sampling: (a) 6, (b) 12, (c) 18, and (d) 24 h after the beginning of the experiment.

middle chamber formed after a half an hour, having a blue bottom layer and a clear top layer. A few very narrow fingers of the triiodide complex solution began to travel up to the upper membrane at the left and right ends of the horizontal cell. We suppose that this phenomenon is a boundary effect.

Especially interesting is the effect of the orientation on the wave shape and velocity. The front velocity is not a maximum when the gravitational force is directly aligned with the direction of propagation (180°). Instead, the velocity is a maximum at 130°. A similar phenomenon was discussed by Davis and Acrivos,³⁷ referring to Boycott,³⁸ who had described the phenomenon of the increased rate of sedimentation of blood corpuscles in a tilted tube. The enhancement of the sedimentation rate results from the fact that particles can only settle down to the bottom in a channel with vertical walls, but particles can also settle onto the upward facing wall in a tilted channel. These particles then form a thin sediment layer that rapidly slides down toward the bottom of the tube under the action of the gravity. In this way, the increase in the settling rate can be attributed to an increase in the surface area available for settling.

In our case the sedimenting “particles” are the parcels formed by the increased density of small regions containing triiodide in the reacted side. In a descending tilted case (e.g., Figure 5, 150°) the increased density causes a downward vertical motion. If these considerations are correct, we should be able to observe the dependence of the wave shape on the orientation in unreactive model experiments. For this reason, we constructed a tubular membrane reactor described in the Figure 2c. For all tubular membrane reactor experiments we used the solution with the same composition as described for the Hele-Shaw-type cell.

First we carried out experiments on the model of the descending propagation, so the triiodide-containing solution (solution 1) was pumped through the upper half of the reactor. A few hours after the beginning the experiment, a descending front formed and propagated very slowly down with a blue color, indicating the presence of the triiodide. The propagation was slower by several orders of magnitudes than in the case of a reactive front. Figure 9 shows a sequence of pictures on the descending front captured by 7-h delay to each other.

The front was relatively slow and diffuse compared to the reactive system, but a slight curvature is seen in Figure 10. After noise reduction and contrast enhancement, we obtained a picture indicating that the front is curved. This observation, except for the time scale, is consistent with the findings in reactive systems that descending fronts show a curved shape (Figure 3b). Moreover, there is a second front that could be observed, but we do not know its origin. The second front is necessarily coupled to the first front and related to different iodide complexes.

In the case of the ascending model system, pumping solution 1 through the bottom chamber of the reactor, we expected to observe a relatively sharp boundary, as seen in front propagation experiments (Figure 3a). The formation of this diffusion front was slower than in the case of the descending model experiment, and probably this is the reason we observed a poorly defined, diffuse front shown in Figure 11a. After image enhancement (Figure 11b) we are convinced that there is no chance to observe

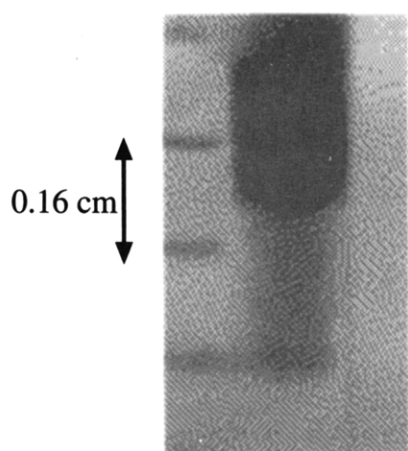


Figure 10. Curvatures of the diffusion front in the reactor shown in Figure 2c.

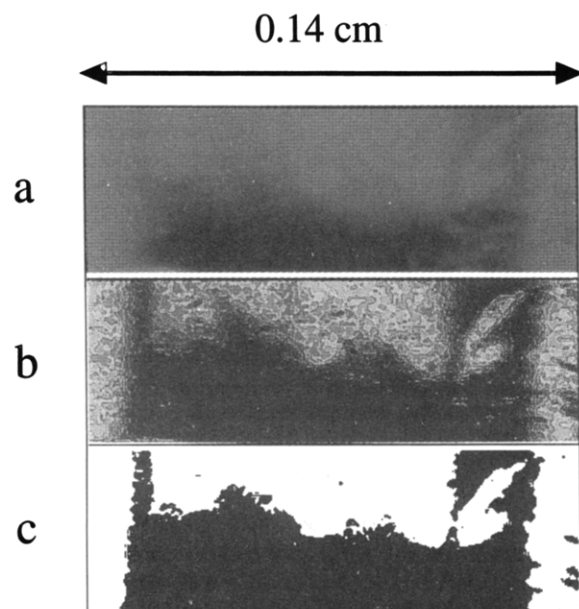
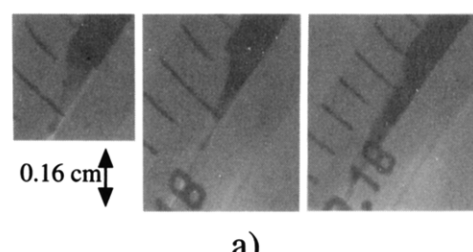


Figure 11. (a) Raw and (b) enhanced images of the shape of the ascending diffusion front. (c) Estimated boundaries of diffuse zone after contrast enhancement and LUT operations. Elapsed time from the beginning of the experiment is 1 h.

a sharply flat front because of the time scale of the diffusion events. Only a diffuse boundary can be estimated on the basis of the experiment (Figure 11c). This is consistent with the mechanism for double-diffusive convection in the diffusive regime (Figure 6b). In the reactive system, the front is sharp because the iodide that is convectively transported across the interface quickly reacts, keeping a sharp front.

We carried out model experiments in tilted tubes, hoping to simulate the Boycott effect found in the reactive system. In a 135° tilted descending case using the same experimental setup as in the descending model system, we observed wave formation and breakup on a time scale of 30–60 min (Figure 12a), which is shorter than the purely vertical propagation time scale of the model system. The distortion of the wave shape is also observed in a 45° tilted ascending model experiment (Figure 12b), but we cannot explain the difference from the reactive system (confer Figure 5d,e).

Sustained Isothermal Multicomponent Systems Based on the Iodide–Iodine–Triiodide–Starch Equilibrium. The model system experiments let us to conclude that diffusion coefficient differences in a fluid reaction system can support spatiotemporal phenomena. In a purely convection-free system it is essential to the formation of Turing structures.³⁹ In the case of our model system, the



a)



b)

Figure 12. Effect of the tube orientation in the tubular membrane reactor fed by unreactive mixtures: (a) wave formation and breakage of descending propagation in the 135° direction to the vertical; (b) wave shape in the case of ascending propagation in the 45° direction to the vertical.

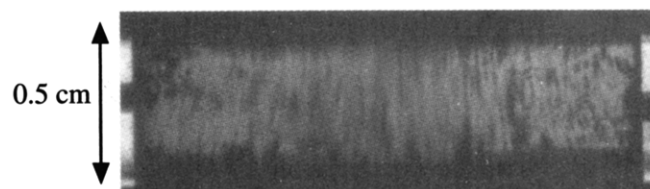


Figure 13. Sustained isothermal multicomponent patterns in the iodine-sulfite system in membrane-equipped Hele-Shaw-type convection cell. Solution for the upper flow chamber: 0.5 M NaNO₃, 0.008 M I₂. Solution for the bottom flow chamber: 8 × 10⁻⁴ M Na₂SO₃, 0.5 M NaNO₃, 0.3 M KI. Initial solution for the midsection: 0.5 M NaNO₃, 0.2 m/v % starch.

continuous influx of iodine precluded the formation of a stable structure. If there is no iodine-consuming process, the structure is limited by thermodynamics. To produce true stationary structures, we added sulfite to consume iodine. After an hour a cloudlike structure (Figure 13) formed and remained stable for several hours. The diffusion of the reacting species (Na₂SO₃, I₂, and KI) through the membrane and solutions and the rate of the iodine–sulfite reaction are able to compete with each other to maintain constant levels of the local concentrations of the triiodide–starch complex.

Comparison with the Iodate–Arsenous Acid System. The phenomena observed in the iodide–nitric acid system qualitatively can be understood as a result of the difference between the diffusion constants for iodide and the triiodide–starch complex. Although the propagation features are strongly determined by the fluid dynamics, the reaction itself is not negligible. For many qualitative features the model experiments provide an adequate answer, but one fact cannot be readily understood. In the iodate–arsenous acid system, in spite of the same relative signs of $\Delta\rho_c$ and $\Delta\rho_T$ as in the iodide–nitric acid system, the wave shapes are reversed in the cases of descending and ascending fronts and the descending front propagates with the same speed as the pure reaction–diffusion front. We believe that starch plays an essential role because its presence can decrease the diffusion coefficient of any species that complexes with it.

The importance of the role of the starch is supported by the work of McManus, who carried out starch concentration dependence experiments in the iodate–arsenous acid system.⁴⁰ He found a 12–30% velocity dependence on the starch concentration for both ascending and descending propagation. Nonetheless, the iodate–arsenous acid system may not exhibit double-

diffusive convection because of its larger thermal gradient that may suppress fingering as in the chlorate–sulfite system.³⁰

Pojman and Epstein classified the possibilities of the convection types based solely on the isothermal and thermal density change. It is necessary to introduce a third factor—the relative size of the diffusion coefficients of the reactants and products. If one diffusion coefficient is only 3 times as large, as with salt and sugar, double-diffusive convection can occur.²¹

Conclusions

Chemical waves are especially well suited for the study of double-diffusive convection because of the high concentration gradients in the fronts that are maintained automatically by the front. Thus, what is normally observed as a transient phenomenon can be observed as a steady process as the front propagates.

We have demonstrated that even in a wave system in which $\Delta\rho_c$ and $\Delta\rho_T$ have the same signs, double-diffusive convection can occur if the diffusion coefficients of reactants and products are sufficiently different. From our experiments with waves and with model reactors, we have shown that the iodide–nitric acid system demonstrates such convection because of the difference in diffusion coefficients for triiodide–starch and iodide. Descending fronts propagate more rapidly than pure reaction–diffusion fronts because of a “salt finger” mechanism that significantly increases the mass transport across the front. Ascending fronts also propagate faster than pure reaction–diffusion fronts, but slower than descending fronts, because the diffusive regime of double-diffusive convection is not as effective at increasing the mass transport as is fingering. This system is more similar to the iron–nitric acid one than to the iodate–arsenous acid system, contradicting the Pojman–Epstein model. For any wave system in which there are species with different diffusion coefficients, this mechanism should be considered, especially if starch is used as an indicator. Polymer systems may be especially susceptible because of the large difference between the diffusion coefficients of the polymer and monomer.

The fronts in the iodide–nitric system exhibit a maximum velocity at 120° to the vertical because of the Boycott effect. Video images demonstrate the change in front shape as a function of tube orientation.

Numerical modeling of these experiments should be done to provide further substantiation for our interpretation.

Acknowledgment. This work was supported by the U.S.–Hungarian Science and Technology Joint Fund (Grant J. F. No. 247/92a), the National Scientific Research Fund of Hungary (OTKA Grant No. F-4024 and No. 1725), and the National Science Foundation’s Mississippi EPSCoR Program.

Supplementary Material Available: Table of velocities at different initial iodide concentrations and different orientations

in a tube (2 pages). Ordering information is given on any current masthead page.

References and Notes

- (1) Zaikin, A. N.; Zhabotinskii, A. M. *Nature* **1970**, *225*, 535–537.
- (2) Winfree, A. T. *Science* **1973**, *181*, 937–939.
- (3) Field, R. J.; Noyes, R. M. *J. Am. Chem. Soc.* **1974**, *96*, 2001–2006.
- (4) Gribshaw, T. A.; Showalter, K.; Banville, D. L.; Epstein, I. R. *J. Phys. Chem.* **1981**, *85*, 2152–2155.
- (5) Bazsa, G.; Epstein, I. R. *J. Phys. Chem.* **1985**, *89*, 3050–3053.
- (6) Hanna, A.; Saul, A.; Showalter, K. *J. Am. Chem. Soc.* **1982**, *104*, 3838–3844.
- (7) Harrison, J.; Showalter, K. *J. Phys. Chem.* **1986**, *90*, 225–226.
- (8) Szirovicza, L.; Nagypál, I.; Boga, E. *J. Am. Chem. Soc.* **1989**, *111*, 2842–2845.
- (9) Ross, J.; Müller, S. C.; Vidal, C. *Science* **1988**, *240*, 460–465.
- (10) Pojman, J. A. *J. Am. Chem. Soc.* **1991**, *113*, 6284–6286.
- (11) Tzalmona, A.; Armstrong, R. L.; Menzinger, M.; Cross, A.; Lemaire, C. *Chem. Phys. Lett.* **1992**, *188*, 457–461.
- (12) Pojman, J. A.; Epstein, I. R.; Nagy, I. *J. Phys. Chem.* **1991**, *95*, 1306–1311.
- (13) Pojman, J. A.; Epstein, I. R.; McManus, T.; Showalter, K. *J. Phys. Chem.* **1991**, *95*, 1299–1306.
- (14) Vasquez, D. A.; Edwards, B. F.; Wilder, J. W. *Phys. Rev. A* **1991**, *43*, 6694–6699.
- (15) Pojman, J. A.; Craven, R.; Khan, A.; West, W. *J. Phys. Chem.* **1992**, *96*, 7466–7472.
- (16) Miike, H.; Müller, S. C.; Hess, B. Interaction of Chemical Waves and Hydrodynamics Flow. In *Cooperative Dynamics in Physical Systems*; 1989; pp 328–329.
- (17) Miike, H.; Müller, S. C.; Hess, B. *Chem. Phys. Lett.* **1988**, *144*, 515–520.
- (18) Nagypál, I.; Bazsa, G.; Epstein, I. R. *J. Am. Chem. Soc.* **1986**, *108*, 3635–3640.
- (19) Pojman, J. A.; Epstein, I. R. *J. Phys. Chem.* **1990**, *94*, 4966–4972.
- (20) Stern, M. E. *Tellus* **1960**, *12*, 172–175.
- (21) Turner, J. S. *Buoyancy Effects in Fluids*; Cambridge University Press: Cambridge, 1973.
- (22) Turner, J. S. *Annu. Rev. Fluid Mech.* **1985**, *7*, 11–44.
- (23) Nason, P.; Schumaker, V.; Halsall, B.; Schwedes, J. *Biopolymers* **1969**, *7*, 241–249.
- (24) Turner, J. S. *Deep-Sea Res.* **1967**, *14*, 599–611.
- (25) Huppert, H. E.; Manins, P. C. *Deep-Sea Res.* **1973**, *20*, 315–333.
- (26) Huppert, H. E.; Turner, J. S. *J. Fluid Mech.* **1981**, *106*, 299–329.
- (27) Linden, P. F. *J. Fluid Mech.* **1971**, *49*, 611–624.
- (28) Linden, P. F. *Deep-Sea Res.* **1973**, *20*, 325–340.
- (29) Avnir, D.; Kagan, M. *Nature* **1984**, *307*, 717.
- (30) Nagy, I. P.; Pojman, J. A. *J. Phys. Chem.* **1993**, *97*, 3443–3449.
- (31) Eckstädt, A. Z. *Anorg. Allg. Chem.* **1902**, *51*, 29.
- (32) Nagy, I. P.; Bazsa, G. *React. Kinet. Catal. Lett.* **1991**, *45*, 4379.
- (33) Bazsa, G.; Epstein, I. R. *Comments Inorg. Chem.* **1986**, *5*, 57–87.
- (34) Pota, G.; Bazsa, G.; Beck, M. T. *Acta Chim. Acad. Hung.* **1982**, *110*, 227.
- (35) Predtechensky, A. A.; McCormick, W. D.; Swift, J. B.; Noszticzius, Z.; Swinney, H. L. *Phys. Rev. Lett.* **1994**, *72*, 218–221.
- (36) Andrea Keresztesy, unpublished data.
- (37) Davis, R. H.; Acuña, A. *Annu. Rev. Fluid Mech.* **1985**, *17*, 91–118.
- (38) Boycott, A. E. *Nature* **1920**, *104*, 532.
- (39) Lengyel, I.; Epstein, I. R. *Science* **1991**, *251*, 650–652.
- (40) McManus, T. J., Ph.D. Thesis, West Virginia University, 1989.